Journal of Materials Chemistry B

PAPER

View Article Online
View Journal | View Issue

Cite this: J. Mater. Chem. B, 2017, 5, 6637

Polymer cloaking modulates the carbon nanotube protein corona and delivery into cancer cells†

Januka Budhathoki-Uprety,[a] Jackson D. Harvey,[ab] Elizabeth Isaac,[b] Ryan M. Williams,[a] Thomas V. Galassi,[ab] Rachel E. Langenbacher[ab] and Daniel A. Heller *[ab]

Received 13th March 2017,
Accepted 12th June 2017

DOI: 10.1039/c7tb00695k

rsc.li/materials-b

Carbon nanotube-based molecular probes, imaging agents, and biosensors in cells and *in vivo* continue to garner interest as investigational tools and clinical devices due to their unique photophysical properties. Surface chemistry modulation of nanotubes plays a critical role in determining stability and interaction with biological systems both *in vitro* and *in vivo*. Among the many parameters that influence the biological fate of nanomaterials, surface charge is particularly influential due to direct electrostatic interactions with components of the cell membrane as well as proteins in the serum, which coat the nanoparticle surface in a protein corona and alter nanoparticle–cell interactions. Here, we modulated functional moieties on a helical polycarbodiimide polymer backbone that non-covalently suspended the nanotubes in aqueous media. By derivatizing the polymer with either primary amine or carboxylic acid side chains, we obtained nanotube complexes that present net surface charges of opposite polarity at physiological pH. Using these materials, we found that the uptake of carbon nanotubes in these cells is highly dependent on charge, with cationic nanotubes efficiently internalized into cells compared to the anionic nanotubes. Furthermore, we found that serum proteins drastically influenced cell uptake of the anionic nanotubes, while the effect was not prominent for the cationic nanotubes. Our findings have implications for improved engineering of drug delivery devices, molecular probes, and biosensors.

Introduction

Single-walled carbon nanotubes (SWCNTs) dispersed as colloidal suspensions are photoluminescent nanomaterials[1] that have generated interest for potential biomedical applications.[2] Their large surface area available for functionalization,[3] stable photoluminescence in the tissue-penetrating near-infrared (NIR) region, and environmental sensitivity make them promising for use as tools for cellular/biomedical imaging,[4–8] photothermal therapy,[9] drug and gene delivery,[10] and optical biosensors for detection of biomolecules *in vitro* and *in vivo*.[11,12] Many of their surface properties can be modulated significantly, which is necessary to counter nanotube hydrophobicity and a strong tendency towards forming aggregates due to large van der Waals interactions in pristine SWCNTs.[13] Both covalent and non-covalent methods are used to render nanotubes soluble in aqueous media.[14,15] Because covalent modifications typically limit their emission, with a few notable exceptions,[16] non-covalent functionalization is often used for optical applications.[4] Non-covalent functionalization of SWCNTs *via* the adsorption of a wide range of molecules such as DNA,[17] enzymes,[18] carbohydrates,[19] proteins and peptides,[20] surfactants,[21] and synthetic polymers[22] on pristine nanotubes preserves the structural, optical, and electrical properties of SWCNTs. These studies also showed that functional coatings on nanotube supramolecular complexes play a critical role in determining stability and biological fate, including cellular uptake/localization[23] and *in vivo* biodistribution.[24] With a growing body of work on nanotube-based molecular probes, imaging agents, and biosensors in cells and *in vivo*, a more complete understanding of the factors that control nanotube uptake into cells is increasingly important.

Uptake of nanomaterials into cells depends on several key factors, including but not limited to, hydrophobicity, surface functional moieties, net charge, size, and shape of nanoparticles.[25] Among these, surface charge is particularly influential due to direct electrostatic interaction with components on the cell membrane[26] as well as serum proteins which coat the nanoparticle surface and alter nanoparticle–cell interactions. Within a class of materials of similar size and shape, a net positive surface charge on nanoparticles correlates with higher cell uptake as compared to respective negatively-charged molecules due to favorable electrostatic interactions between the positive

[a] Memorial Sloan Kettering Cancer Center, New York, New York 10065, USA. E-mail: hellerd@mskcc.org
[b] Weill Cornell Medical College, New York, New York 10065, USA

† Electronic supplementary information (ESI) available: Further characterization, materials, methods and additional figures. See DOI: 10.1039/c7tb00695k

charge on the material and the negative charge on the cell surface.[27] SWCNTs are a unique class of nanomaterial with a high aspect ratio whose cell internalization has been reported to take place both by energy-dependent endocytosis[28] or passive direct membrane penetration.[29] Most non-covalently modified SWCNTs investigated in mammalian cells are negatively charged (with a few exceptions) due to their surface coating with DNA, protein, enzymes, phospholipids, and biocompatible surfactants. This limits direct comparisons of cell internalization with an oppositely-charged analogue without significant structural or chemical changes. Charge-dependent uptake in specific cell lines appears to occur with a wide range of nanomaterials, including gold nanoparticles, polystyrene nanoparticles, and quantum dots, among others.[27]

In serum and blood, nanomaterials without protective modifications are often opsonized, forming a dynamic corona, which influences cellular uptake and *in vivo* studies.[30,31] The protein corona is formed as a result of electrostatic and hydrophobic interactions between nanomaterials and proteins. The net surface charge on a nanomaterial influences protein corona formation *via* conformational changes of the adsorbed serum proteins that influences the nanomaterial–cell interaction, cell internalization,[32] biological activity, and molecular targeting of nanomaterials.[33] Thus, a complete understanding of serum adsorption and how it can be controlled is critical in evaluating the biological fate of nanomaterials both *in vitro* and *in vivo*. Serum conditions can be transiently modulated *in vitro* to study internalization of nanomaterials, providing a model system in which these interactions can be studied. DNA-functionalized SWCNTs, which are intrinsically negatively-charged, exhibit non-specific adsorption of serum proteins, predominantly albumin, during such *in vitro* studies.[34] Additionally, a bovine serum albumin (BSA) coating on the surface of pristine SWCNTs results in water soluble protein–SWCNT complexes.[35] However, no information is available on the effect of serum proteins on cellular uptake of structurally comparable non-covalently functionalized SWCNTs that differ in net surface charge.

Here, we investigated the role of surface functional moieties with net opposite surface charges on nanotube internalization into cells. We non-covalently functionalized SWCNTs by encapsulation in helical polycarbodiimide polymers functionalized with either primary amine (amine-SWCNT) or carboxylic acid (carboxy-SWCNT) side chains. These two side chains were chosen not only for their intrinsic charge differences but also for their biological relevance and amenability to further derivation which could facilitate future probe or biosensor development. These polymers have very similar physical properties, differing only in one of the pendant functional groups and net surface charge from the polymer side chains, providing a clean system in which the effects of charge differences can be isolated from large structural differences. The polymer–nanotube assembly is driven by π–π interactions between the graphitic carbon nanotube surface and the phenyl side groups on the polymers. Aqueous solubility is conferred from hydrophilic/ionizable moieties. Previously, we reported that polycarbodiimide polymers can effectively solubilize SWCNTs in aqueous media, resulting in photoluminescent complexes that are stable under ambient conditions for several months.[22] Here, we studied the cellular uptake of select polymer–SWCNT complexes *in vitro* using the commonly studied HeLa cell line as a representative model. This work also investigates the effect of serum proteins on carbon nanotube uptake into cells. Given the importance of epithelial cells in many types of cancer,[36] the knowledge gained from this study provides insight into developing carbon nanotube-based molecular probes and sensors to study many epithelial-derived cancers. We found that the uptake of carbon nanotubes in these cells under identical incubation conditions is highly-dependent on nanotube surface chemistry. Furthermore, we also found that serum proteins markedly influence cell uptake of anionic carboxy-SWCNTs and the uptake can be modulated, while the effect was not prominent for cationic amine-SWCNTs. The findings from this work have implications for improved engineering of targeted molecular probes, nanosensors, and drug delivery devices.

Results and discussion

Synthesis and characterization of polymer-cloaked SWCNTs

We synthesized helical polycarbodiimide polymers as previously described[37] and incorporated a phenyl pendant group and either amine or carboxylic acid functionalities (Fig. S1, ESI†). Primary amine (–NH_2) or carboxylic acid (–COOH) groups were chosen to mimic the side chain functionalities of lysine and glutamic acid, respectively. The functional groups are ionized under physiological conditions (pH 7.4) and confer a net surface charge of opposite polarity. We suspended SWCNTs with these polycarbodiimides (Fig. 1a) *via* a previously described method.[22,23] The nanotubes are encapsulated in the polymers *via* π–π interactions between the aromatic groups on the polymer side chains and the graphitic surface of carbon nanotubes. The functional side chains were exposed on the polymer–SWCNTs supramolecular complexes and facilitated aqueous solubility and colloidal stability of the complexes.[22] The charged functional groups were situated on the same polymer backbone so that physicochemical parameters outside of charge remain the same. The absorption and photoluminescence on the polymer–SWCNT complexes in water showed distinct absorption bands of dispersed nanotubes in the visible to near-infrared (Vis–NIR) spectral window (Fig. 1b) and a bright NIR photoluminescence (Fig. 1c), characteristic of SWCNTs produced by the HiPCO method and well-dispersed in solution. The surface charges (ζ-potential measured in water) on amine- and carboxy-SWCNT complexes were 52.8 ± 1.6 mV and −66.8 ± 1 mV, respectively (Fig. 1d), consistent with ionized surface functional moieties. The nanotube morphology was characterized by atomic force microscopy (AFM). The AFM image analysis (Fig. S2, ESI†) showed singly-dispersed nanotubes with comparable sizes (amine-SWCNTs, mean length 240 nm, n = 715; and carboxy-SWCNTs, mean length 177 nm, n = 723). However, the observed differences in length distribution may have arisen *via* differential adherence of nanotubes on the mica surface, due to their different net charges. The polymer–SWCNT suspensions were stable at room temperature for several months (*ca.* 24 months)

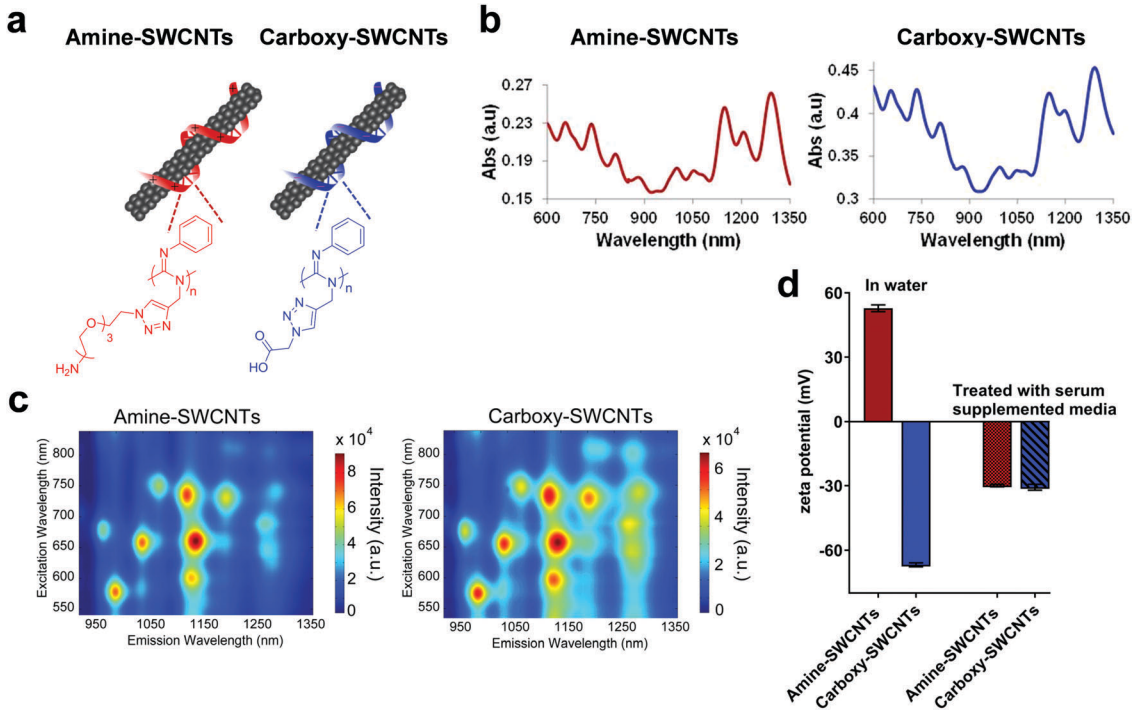

Fig. 1 Characterization of polycarbodiimide polymer–SWCNT complexes. (a) Assembly of amine- and carboxy-SWCNTs, (b) Vis–NIR absorption spectra of polymer–SWCNT complexes in water, (c) photoluminescence excitation/emission map of polymer–SWCNT complexes in water, (d) surface charge (ζ-potential) measurements on polymer–SWCNT complexes in water and upon treatment with cell culture media supplemented with 10% serum.

and remained individualized, as determined from UV-Vis-NIR absorbance and photoluminescence measurements.

The polymer–SWCNTs were also labeled with fluorescein or Alexa 488 to provide a visible fluorophore on the polymer–SWCNT complex (Fig. S3, ESI†). HeLa cells were incubated in the presence of fluorophore-labeled polymer–SWCNTs, washed, and imaged using a single microscope equipped with two different cameras (details in experimental section) to visualize both the NIR photoluminescence of SWCNTs and visible fluorophores of the same view area. The intrinsic NIR photoluminescence from the SWCNTs co-localized with the visible fluorophore on the encapsulating polymers (Fig S4, ESI†), suggesting that these polymer–SWCNT supramolecular complexes maintained their stability in cells.

Differential uptake of SWCNTs in cells

We incubated HeLa cells in the presence of polymer–SWCNT complexes under standard cell culture conditions (DMEM supplemented with fetal bovine serum (10%)). The amine-SWCNTs were found to associate with the cell surface within minutes and internalize over the course of a few hours at a substantially higher rate than carboxy-SWCNTs (Fig. 2a). This charge-dependent behavior of nanotubes in cells is consistent with other nanomaterials.[38] The apparent charge-dependent uptake of nanotubes cannot be fully explained by electrostatic interactions directly with cells due to the presence of serum proteins in the cell culture media and possible effects of the protein corona. In serum-containing media, we found that polymer–nanotube complexes lost their initial charge identities and displayed nearly identical surface potentials (~−30 mV, Fig. 1d), suggesting protein corona formation on both types of nanotube complexes regardless of their initial charge identities. Such surface charge modulation in a complex protein environment has been observed in other classes of nanomaterials.[39] However, the cell uptake behavior of these two types of polymer–nanotube complexes was drastically different under identical incubation conditions. The differences are likely due to differing protein adsorption/desorption rates[40] due to the different electrostatic natures of amine- and carboxy-SWCNTs.

We performed cell viability studies to investigate the toxicity of these materials in cells. Cytotoxicity of these polymer–SWCNTs complexes were assessed as a function of the polymer dispersant, concentration, and exposure time using a propidium iodide assay (Tali Viability Kit – Dead cell Red). These assays showed virtually no changes in viability upon incubation of the cells up to 48 h in the presence of 0.2–1.0 mg L^{-1} polymer–nanotubes (Fig. 2b). Despite substantially higher cell uptake of amine-SWCNTs compared to carboxy-SWCNTs, cell viability appears to be similar. Since surface functionalization can modulate the toxicity of nanotubes,[41] the attenuated cytotoxicity of polycarbodiimide–SWCNTs may be attributed to the cloaking of the nanotubes in polymers functionalized with moieties that confer aqueous solubility and biocompatibility. These results suggest that polymer–SWCNTs were non-toxic to cells under the experimental conditions, irrespective of their surface chemistry and net charge.

Energy dependence of cell uptake

To study the cellular uptake mechanism of these polymer–SWCNTs, we incubated cells in serum-supplemented media in

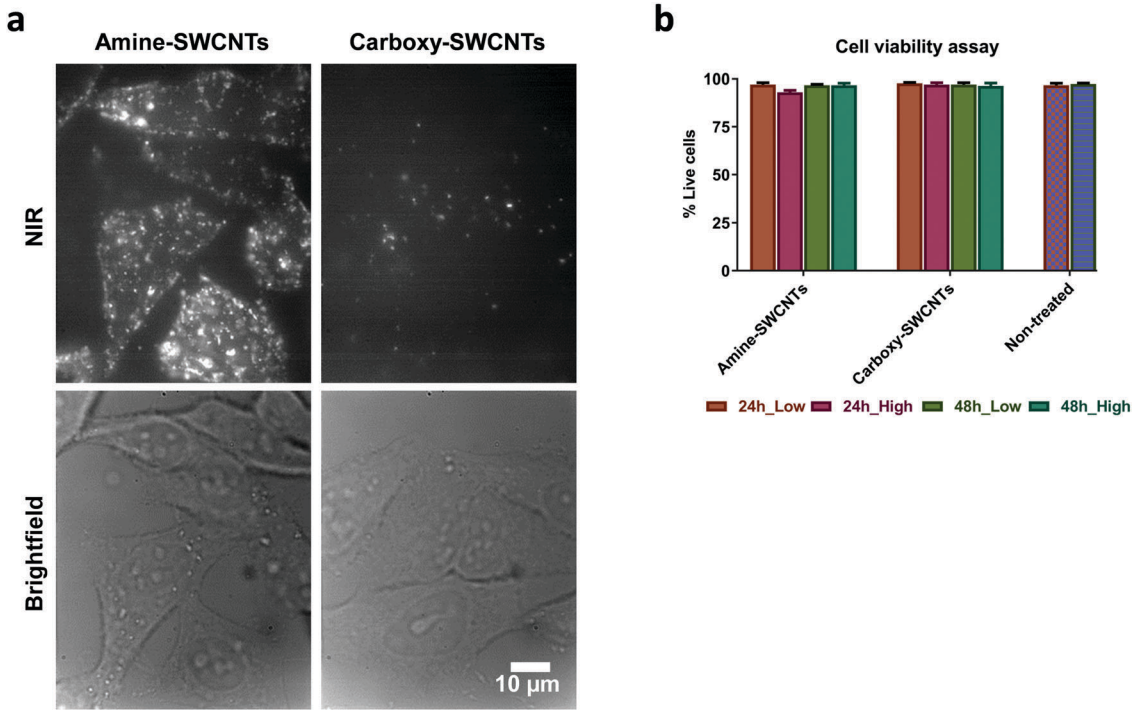

Fig. 2 Polymer–SWCNT interactions with HeLa cells. (a) Near-infrared emission of polymer–SWCNTs in/on HeLa cells. (b) Cell viability assay as a function of incubation time (24–48 h) and concentration of polymer–SWCNTs at 0.2 mg L^{-1} (low) and 1.0 mg L^{-1} (high).

the presence of nanotubes at 4 °C to inhibit energy-dependent uptake. A substantial reduction in cell-associated nanotubes with virtually no internalization was observed at 4 °C compared to 37 °C (Fig. S5, ESI†). The energy-dependent endocytosis of these nanotubes was independent of surface functionalization, consistent with other non-covalent complexes of SWCNTs,[42] and they did not appear to undergo a membrane penetration process *via* the "nanoneedle" mechanism observed in covalently-modified cationic nanotubes.[43]

Effect of serum proteins on cell uptake

In order to discern whether differential uptake of polymer–SWCNTs is intrinsic or due to the characteristics of protein corona formation, we incubated HeLa cells with polymer–SWCNTs in serum-free cell culture media (SFM, DMEM supplemented with antibiotics, HEPES buffer and glutamine) to avoid potential protein corona formation. The cells were washed thoroughly to remove free nanotubes, and emission from visible fluorophores conjugated to the polymer in the complexes was measured with a fluorescence plate reader. No significant difference in total emission intensity from cells incubated with amine-SWCNTs in complete media *versus* SFM was observed (Fig. 3a). However, a marked serum-dependence was observed for carboxy-SWCNTs, with a substantial increase in cell-associated polymer–nanotubes fluorescence under serum-free incubation conditions (Fig. 3b). The visible fluorescence emission measured in a plate reader includes light from both internalized and surface-adsorbed nanotubes. Cell imaging is often necessary to confirm the internalization. To distinguish internalized nanotubes from cell surface-adsorbed nanotubes, cells were trypsinized, rinsed of free nanotubes, re-plated, and incubated for an additional 24 hours to allow complete internalization of nanotubes. The live-cell imaging in the NIR spectral window confirmed that the nanotubes were completely internalized into cells. The relative amounts of nanotubes taken up by cells under serum *vs.* serum free conditions were consistent with data obtained by fluorescence plate reader measurements of the fluorophores bound to the nanotube complexes (Fig. 3c), suggesting that the cell uptake of the nanotubes was directly proportional to the amount associated with the cells. We verified that cell culture media supplemented with serum (10%) did not quench the intrinsic NIR fluorescence on carboxy-SWCNTs and the visible fluorescence on the complexes (Fig. S6, ESI†).

We performed experiments to evaluate the effect of albumin proteins, using bovine serum albumin (BSA), on cell internalization of carboxy-SWCNTs. Although serum is a complex mixture of biomolecules, we used albumin as it is the most abundant protein in the serum of all vertebrates.[44] Cells were cultured under standard conditions and placed in serum-free media (SFM) supplemented with varying concentrations of BSA and a constant concentration of carboxy-SWCNTs for one hour. The presence of BSA in the cell culture media inhibited uptake of nanotubes in a concentration-dependent manner (Fig. 4a and b), consistent with other anionic nanoparticles.[45]

To understand whether the supramolecular complexes of polymer–nanotubes with BSA were stable during uptake into cells, we incubated HeLa cells in the presence of carboxy-SWCNTs and a low concentration (0.1 mg mL^{-1}) of fluorophore-labeled (Texas Red) BSA to visualize the simultaneous uptake of carboxy-SWCNTs and BSA. Fig. 5 shows confocal microscope images of

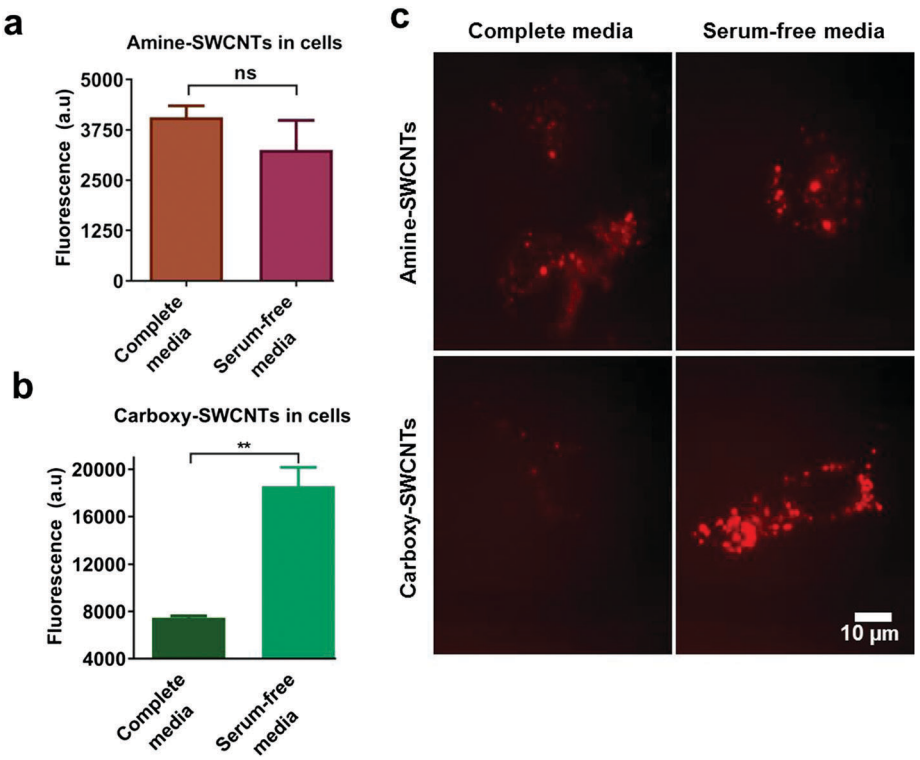

Fig. 3 Effect of serum on uptake of polymer-SWCNTs. (a) Fluorescence emission from HeLa cell-associated (a) amine-SWCNTs, (b) carboxy-SWCNTs. Fluorescence from visible fluorophore-labeled nanotubes was measured in a plate reader. (c) Representative NIR images of internalized SWCNTs in HeLa cells. Experiments were performed in triplicate. The significance was calculated using a two-tailed, unpaired *t* test. $p < 0.05$ is significant.

nanotubes partially co-localized with BSA. Analysis of total near-infrared punctae (~13 384) showed that ~22% of punctae co-localized with BSA in cells.

Conclusions

We developed modular water-soluble carbon nanotube complexes using helical polycarbodiimides, a polymer system that allowed the tuning of surface functional moieties without large structural changes. Using amine and carboxylic acid functionalized polycarbodiimides that conferred net opposite charges at physiological pH, we investigated how the changes in polymer charge mediated the efficiency of uptake of nanotubes into cervical cancer cells. We found that cellular uptake of these polymer–nanotubes is highly dependent on their surface functional moieties, resulting in a higher uptake of amine-nanotubes as compared to carboxy-nanotubes. Given the fact that nanotubes encountered serum proteins in cell culture media, we also studied the effect of serum protein opsonization in nanotube delivery into these cells. We found that serum proteins have a profound impact on nanotube delivery into cells and their effects can be tuned based on nanomaterial surface chemistry. Our studies showed that efficient delivery of carbon nanotubes into epithelial cancer cells (*e.g.*; HeLa) can be achieved *via* surface chemistry modulation. Also, the functional groups are biocompatible conjugation sites that can be exploited to develop specific molecular probes and biosensors. These findings have implications for designing drug delivery strategies, optical probes, and biosensors for cell-based assays.

Experimental

Preparation of polymer–nanotube complexes

Aqueous suspension of polymer-suspended single-walled carbon nanotubes were prepared as reported previously.[22] In brief, as-produced HiPco SWCNTs (Unidym, Lot # R1901, 2 mg) were added to an aqueous suspension (1 mL) of polycarbodiimide polymer functionalized with either primary amine side chains (amine-polymer, 5 mg mL^{-1}, pH ~ 3) or functionalized with carboxylic acid side chains (carboxy-polymer, 5 mg mL^{-1}, pH ~ 9). The mixtures were sonicated by probe-tip for 20 minutes (750 W, 20 kHz, 40% Amplitude, SONICS VibraCell) at low temperature using a CoolRack M30 PF (BioCision), precooled at −20 °C. The mixtures were centrifuged twice for 1 h at 30 000 rcf at 20 °C (centrifuge 5430 R, Eppendorf), and pellets were discarded to remove unsuspended material. The supernatants were filtered through centrifugal filter units (100 kDa MWCO, Amicon Ultracel, Merck Millipore Ltd) four times to remove small molecules and excess polymer. Removal of acid/base from the suspension was confirmed with litmus paper. Ultrapure water (18.2 mΩ) was used for all aqueous solutions. The suspensions were characterized by ultraviolet-visible-near-infrared (UV-VIS-NIR) absorbance (Jasco V-670, Tokyo, Japan), NIR fluorescence spectroscopies (Isoplane spectrograph (Princeton Instruments)), zeta potential

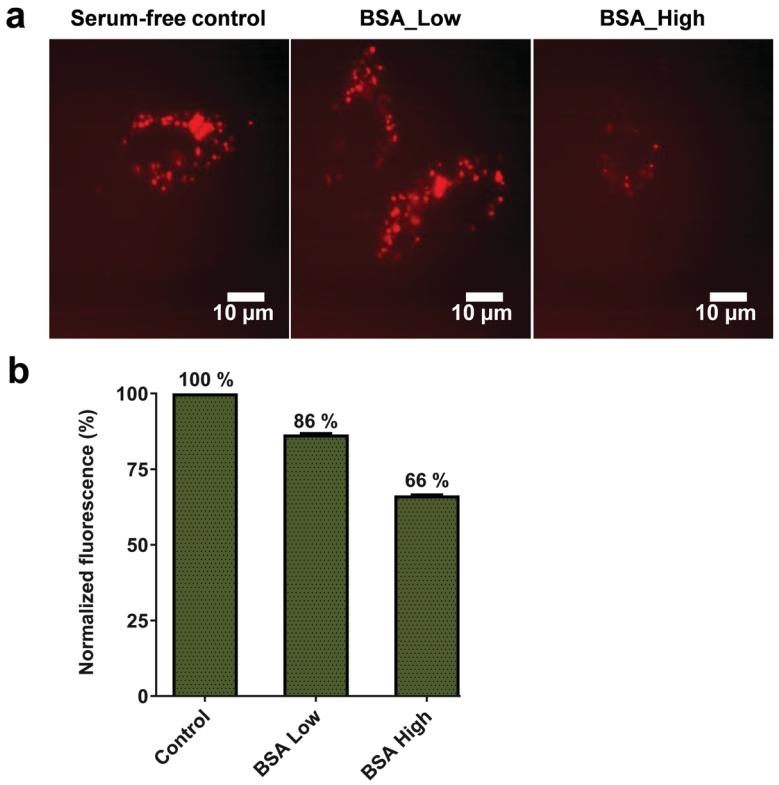

Fig. 4 Competitive inhibition by bovine serum albumin protein on the cellular uptake of carboxy-SWCNTs. (a) NIR emission of SWCNTs incubated with HeLa cells in the absence of BSA, under low concentration of BSA (BSA_low, 0.2 mg mL^{-1}), and high concentration of BSA (BSA_High, 10 mg mL^{-1}). (b) Normalized Alexa 488 emission of fluorophore-bound Carboxy-SWCNTs incubated at various concentration of BSA, measured with a fluorescence plate reader.

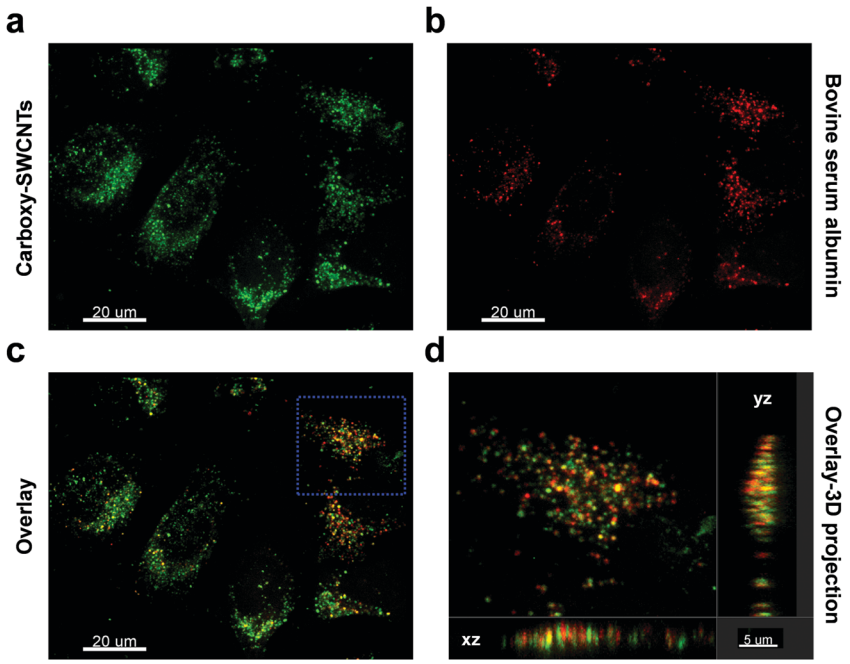

Fig. 5 Confocal microscopy images of HeLa cells showing internalized nanotube complexes in green (a) and bovine serum albumin in red (b). Cells were treated simultaneously with carboxy-SWCNTs and fluorophore (Texas-red)-labeled bovine serum albumin. Panel c is the overlay image from panel a and b, showing co-localization in yellow. Panel d shows a 3D projection of the boxed area on image c with *x*–*z* projections in the bottom margin and *y*–*z* in the right margin.

(surface charge) measurements (Zetasizer nano zs, Malvern), and atomic force microscopy (Asylum Research MFP-3D-Bio instrument was used with an Olympus AC240TS AFM probe in AC mode). The resulting dark suspensions of polymer–nanotube complexes were stored at room temperature.

Cell culture and nanotube uptake

HeLa cells were purchased from American Type Culture Collection (ATCC) and cultured in media (Dulbecco's Modified Eagle Medium, DMEM) supplemented with heat inactivated Fetal Bovine Serum (FBS), penicillin–streptomycin (10 000 U mL^{-1}), glutamine, and (4-(2-hydroxyethyl)-1-piperazineethanesulfonic acid, 1 M) HEPES buffer at 10%, 1%, 1%, and 2.5% (v/v) respectively at 37 °C in humidified air containing 5% CO_2. All reagents were purchased from Life Technologies. Cells were washed, trypsinized, and plated onto a 24 well clear bottom dishes or a 35 mm glass bottom dish (MatTek, Ashland, MA) to obtain 70–80% confluence. After 24 h, conditioned media from cell culture was removed and replaced with fresh media. Aqueous suspension of polymer–nanotubes ($\sim$4 mg L^{-1} nanotubes stock sample) were initially diluted in cell culture media (100 μL) and then added to cells to a final concentration of 0.1–1 mg L^{-1} of nanotubes in media. Cells were incubated with this solution for the time period specified in the text, washed with PBS (w/o Ca^{++}/Mg^{++}) three times, incubated in fresh cell culture media, and imaged. The following conditions (nanotube concentration and incubation time period) were employed in specified experiments: (1) Fig. 2a, cells were incubated for 30 minutes in the presence of polymer–nanotubes (amine-SWCNTs, 0.1 mg L^{-1} and carboxy-SWCNTs 0.5 mg L^{-1}). (2) Fig. 3a, cells were incubated for 60 minutes in the presence of polymer–nanotubes (amine-SWCNTs, 0.2 mg L^{-1} and carboxy-SWCNTs 0.8 mg L^{-1}). After fluorescence measurements in a plate reader (Tecan, Switzerland), cells were washed, trypsinized, and plated into a 35 mm glass bottom dish (MatTek) and imaged after 24 h incubation (Fig. 3b). (3) Fig. 4, cells were incubated for 60 minutes in the presence of polymer–nanotubes (carboxy-SWCNTs 0.8 mg L^{-1}). (4) Fig. 5, cells were incubated for 60 minutes in the presence of polymer–nanotubes (carboxy-SWCNTs 0.25 mg L^{-1}), washed with PBS and fixed (4% paraformaldehyde, 30 minutes at room temperature) prior to imaging.

Live cell NIR imaging

The near-infrared photoluminescence imaging of the cells was performed using a fluorescence microscope equipped with 2D InGaAs array camera (Photon *etc.*) under 730 nm excitation and 0.2 s exposure, as described.[46,47] A 100X (1.40 NA) oil objective was used to collect broadband NIR images (900–1600 nm) of nanotubes in cells using the same microscope without the hyperspectral functionalities. Images were processed using ImageJ software (NIH).

Confocal imaging of fluorophore-labeled nanotubes

HeLa cells were incubated in the serum-free cell culture media containing carboxy-SWCNTs (0.25 mg L^{-1} nanotubes) and BSA (Texas red-labeled BSA, 0.1 mg mL^{-1}) for 60 min. The cells were washed with PBS three times and incubated under standard conditions in fresh media (with 10% FBS) overnight. Cells were washed with PBS and fixed in 4% paraformaldehyde for 30 minutes at room temperature, and imaged with a confocal laser scanning microscope (Leica SP8) with a 63X glycerol immersion objective. Images were processed using Bitplane Imaris 8.0.2 software.

Acknowledgements

This work was supported in part by the NIH New Innovator Award (DP2-HD075698), the Cancer Center Support Grant (P30 CA008748), the Anna Fuller Fund, the Louis V. Gerstner Jr. Young Investigator's Fund, the Frank A. Howard Scholars Program, the Honorable Tina Brozman Foundation for Ovarian Cancer Research, the Expect Miracles Foundation – Financial Services Against Cancer, Cycle for Survival, the Alan and Sandra Gerry Metastasis Research Initiative, Mr William H. Goodwin and Mrs Alice Goodwin and the Commonwealth Foundation for Cancer Research, the Experimental Therapeutics Center, the Imaging & Radiation Sciences Program, and the Center for Molecular Imaging and Nanotechnology of Memorial Sloan Kettering Cancer Center. J. B. was supported by the Tow Foundation Postdoctoral Fellowship, Center for Molecular Imaging and Nanotechnology at MSKCC, R. M. W. was supported by the Ovarian Cancer Research Fund – Ann Schreiber Mentored Investigator Award (370463). The authors would like to thank M. B. Brendel, Y. Romin, and V. Boyko for technical assistance, and core facilities at Memorial Sloan Kettering Cancer Center: the Molecular Cytology Core Facility for AFM imaging (Core Grant P30 CA008748), and the Analytical Core Facility for Nuclear Magnetic Resonance, FTIR, and High Resolution Mass Spectroscopies.

References

1 M. J. O'Connell, S. M. Bachilo, C. B. Huffman, V. C. Moore, M. S. Strano, E. H. Haroz, K. L. Rialon, P. J. Boul, W. H. Noon, C. Kittrell, J. P. Ma, R. H. Hauge, R. B. Weisman and R. E. Smalley, *Science*, 2002, **297**, 593–596.
2 Z. Liu, S. Tabakman, K. Welsher and H. Dai, *Nano Res.*, 2009, **2**, 85–120.
3 C. J. Serpell, R. N. Rutte, K. Geraki, E. Pach, M. Martincic, M. Kierkowicz, S. De Munari, K. Wals, R. Raj, B. Ballesteros, G. Tobias, D. C. Anthony and B. G. Davis, *Nat. Commun.*, 2016, **7**, 13118.
4 S. Kruss, A. J. Hilmer, J. Zhang, N. F. Reuel, B. Mu and M. S. Strano, *Adv. Drug Delivery Rev.*, 2013, **65**, 1933–1950.
5 N. Fakhri, A. D. Wessel, C. Willms, M. Pasquali, D. R. Klopfenstein, F. C. MacKintosh and C. F. Schmidt, *Science*, 2014, **344**, 1031–1035.
6 P. V. Jena, Y. Shamay, J. Shah, D. Roxbury, N. Paknejad and D. A. Heller, *Carbon*, 2016, **97**, 99–109.
7 P. Cherukuri, S. M. Bachilo, S. H. Litovsky and R. B. Weisman, *J. Am. Chem. Soc.*, 2004, **126**, 15638–15639.

8 G. S. Hong, S. Diao, J. L. Chang, A. L. Antaris, C. X. Chen, B. Zhang, S. Zhao, D. N. Atochin, P. L. Huang, K. I. Andreasson, C. J. Kuo and H. J. Dai, *Nat. Photonics*, 2014, **8**, 723–730.
9 H. K. Moon, S. H. Lee and H. C. Choi, *ACS Nano*, 2009, **3**, 3707–3713.
10 Z. Liu, K. Chen, C. Davis, S. Sherlock, Q. Z. Cao, X. Y. Chen and H. J. Dai, *Cancer Res.*, 2008, **68**, 6652–6660.
11 N. M. Iverson, P. W. Barone, M. Shandell, L. J. Trudel, S. Sen, F. Sen, V. Ivanov, E. Atolia, E. Farias, T. P. McNicholas, N. Reuel, N. M. Parry, G. N. Wogan and M. S. Strano, *Nat. Nanotechnol.*, 2013, **8**, 873–880.
12 J. D. Harvey, P. V. Jena, H. A. Baker, G. H. Zerze, R. M. Williams, T. V. Galassi, D. Roxbury, J. Mittal and D. A. Heller, *Nat. Biomed. Eng.*, 2017, **1**, 0041.
13 A. Battigelli, C. Menard-Moyon, T. Da Ros, M. Prato and A. Bianco, *Adv. Drug Delivery Rev.*, 2013, **65**, 1899–1920.
14 P. Singh, S. Campidelli, S. Giordani, D. Bonifazi, A. Bianco and M. Prato, *Chem. Soc. Rev.*, 2009, **38**, 2214–2230.
15 B. I. Kharisov, O. V. Kharissova and A. V. Dimas, *RSC Adv.*, 2016, **6**, 68760–68787.
16 Y. Piao, B. Meany, L. R. Powell, N. Valley, H. Kwon, G. C. Schatz and Y. Wang, *Nat. Chem.*, 2013, **5**, 840–845.
17 M. Zheng, A. Jagota, E. D. Semke, B. A. Diner, R. S. McLean, S. R. Lustig, R. E. Richardson and N. G. Tassi, *Nat. Mater.*, 2003, **2**, 338–342.
18 P. W. Barone, S. Baik, D. A. Heller and M. S. Strano, *Nat. Mater.*, 2005, **4**, 86–92.
19 B. K. Gorityala, J. M. Ma, X. Wang, P. Chen and X. W. Liu, *Chem. Soc. Rev.*, 2010, **39**, 2925–2934.
20 D. A. Heller, G. W. Pratt, J. Q. Zhang, N. Nair, A. J. Hansborough, A. A. Boghossian, N. F. Reuel, P. W. Barone and M. S. Strano, *Proc. Natl. Acad. Sci. U. S. A.*, 2011, **108**, 8544–8549.
21 R. Rastogi, R. Kaushal, S. K. Tripathi, A. L. Sharma, I. Kaur and L. M. Bharadwaj, *J. Colloid Interface Sci.*, 2008, **328**, 421–428.
22 J. Budhathoki-Uprety, P. V. Jena, D. Roxbury and D. A. Heller, *J. Am. Chem. Soc.*, 2014, **136**, 15545–15550.
23 J. Budhathoki-Uprety, R. E. Langenbacher, P. V. Jena, D. Roxbury and D. A. Heller, *ACS Nano*, 2017, **11**, 3875–3882.
24 Z. Liu, C. Davis, W. B. Cai, L. He, X. Y. Chen and H. J. Dai, *Proc. Natl. Acad. Sci. U. S. A.*, 2008, **105**, 1410–1415.
25 A. M. Bannunah, D. Vllasaliu, J. Lord and S. Stolnik, *Mol. Pharmaceutics*, 2014, **11**, 4363–4373.
26 D. Roxbury, P. V. Jena, Y. Shamay, C. P. Horoszko and D. A. Heller, *ACS Nano*, 2016, **10**, 499–506.
27 E. Frohlich, *Int. J. Nanomed.*, 2012, **7**, 5577–5591.
28 G. Hong, J. Z. Wu, J. T. Robinson, H. Wang, B. Zhang and H. Dai, *Nat. Commun.*, 2012, **3**, 700.
29 S. Kraszewski, A. Bianco, M. Tarek and C. Ramseyer, *PLoS One*, 2012, **7**, e40703.
30 X. N. Cai, R. Ramalingam, H. S. Wong, J. P. Cheng, P. Ajuh, S. H. Cheng and Y. W. Lam, *J. Nanomed. Nanotechnol.*, 2013, **9**, 583–593.
31 I. Lynch, A. Salvati and K. A. Dawson, *Nat. Nanotechnol.*, 2009, **4**, 546–547.
32 C. C. Fleischer and C. K. Payne, *Acc. Chem. Res.*, 2014, **47**, 2651–2659.
33 D. Dutta, S. K. Sundaram, J. G. Teeguarden, B. J. Riley, L. S. Fifield, J. M. Jacobs, S. R. Addleman, G. A. Kaysen, B. M. Moudgil and T. J. Weber, *Toxicol. Sci.*, 2007, **100**, 303–315.
34 C. Salvador-Morales, E. Flahaut, E. Sim, J. Sloan, M. L. Green and R. B. Sim, *Mol. Immunol.*, 2006, **43**, 193–201.
35 B. D. Holt, K. N. Dahl and M. F. Islam, *Small*, 2011, **7**, 2348–2355.
36 K. Polyak and R. A. Weinberg, *Nat. Rev. Cancer*, 2009, **9**, 265–273.
37 J. Budhathoki-Uprety and B. M. Novak, *Macromolecules*, 2011, **44**, 5947–5954.
38 D. Huhn, K. Kantner, C. Geidel, S. Brandholt, I. De Cock, S. J. H. Soenen, P. R. Gil, J. M. Montenegro, K. Braeckmans, K. Mullen, G. U. Nienhaus, M. Klapper and W. J. Parak, *ACS Nano*, 2013, **7**, 3253–3263.
39 R. M. Williams, J. Shah, B. D. Ng, D. R. Minton, L. J. Gudas, C. Y. Park and D. A. Heller, *Nano Lett.*, 2015, **15**, 2358–2364.
40 M. P. Monopoli, C. Aberg, A. Salvati and K. A. Dawson, *Nat. Nanotechnol.*, 2012, **7**, 779–786.
41 J. P. Cheng, K. A. S. Fernando, L. M. Veca, Y. P. Sun, A. I. Lamond, Y. W. Lam and S. H. Cheng, *ACS Nano*, 2008, **2**, 2085–2094.
42 P. N. Yaron, B. D. Holt, P. A. Short, M. Losche, M. F. Islam and K. N. Dahl, *J. Nanobiotechnol.*, 2011, **9**, 45.
43 K. Kostarelos, L. Lacerda, G. Pastorin, W. Wu, S. Wieckowski, J. Luangsivilay, S. Godefroy, D. Pantarotto, J. P. Briand, S. Muller, M. Prato and A. Bianco, *Nat. Nanotechnol.*, 2007, **2**, 108–113.
44 A. M. Merlot, D. S. Kalinowski and D. R. Richardson, *Front. Physiol.*, 2014, **5**, 299.
45 C. C. Fleischer, U. Kumar and C. K. Payne, *Biomater. Sci.*, 2013, **1**, 975–982.
46 T. V. Galassi, P. V. Jena, D. Roxbury and D. A. Heller, *Anal. Chem.*, 2017, **89**, 1073–1077.
47 D. Roxbury, P. V. Jena, R. M. Williams, B. Enyedi, P. Niethammer, S. Marcet, M. Verhaegen, S. Blais-Ouellette and D. A. Heller, *Sci. Rep.*, 2015, **5**, 14167, DOI: 10.1038/srep14167.

